Journal of Operation and Automation in Power Engineering
Vol. 5, No. 2, Dec. 2017, Pages: 151-162
http://joape.uma.ac.ir

Distributed Multi-Agent Load Frequency Control for a Large-Scale Power System Optimized by Grey Wolf Optimizer

M. Olyaee, A. Akbarimajd [*], *H. Shayeghi, B. Sobhani*

Department of Electrical Engineering, University of Mohaghegh Ardabili, Ardabil, Iran..

Abstract- *This paper aims to design an optimal distributed multi-agent controller for load frequency control and optimal power flow purposes. The controller parameters are optimized using Grey Wolf Optimization (GWO) algorithm. The designed optimal distributed controller is employed for load frequency control in the IEEE 30-bus test system with six generators. The controller of each generator is considered as one agent. The controllers of agents are implemented in a distributed manner that is control rule of each agent depends on the agents' own state and the states of their neighbors. Three other types of controllers including centralized controller, decentralized controller, and optimal centralized controller are considered for comparison. The performances of decentralized and distributed controllers are compared with two centralized controllers. In the optimal centralized controller and optimal distributed controller, the objective function is considered to achieve the objective of load frequency control as well as minimize power generation. Simulation results using MATLAB/SIMULINK show that although there is no global information of system in the optimal distributed controller, it has suitably reduced the frequency deviation. Meanwhile the power is optimally generated in the three scenarios of load increasing, load reduction and generator outage.*

Keyword: Load frequency control, Distributed controller, Optimal power flow, Grey wolf optimizer, Multi-agent systems.

1. INTRODUCTION

The main purpose of automatic generation control (AGC) is to stabilize the general system generation against load changing so that the scheduled frequency is preserved even with power exchange between neighboring systems. Any inequality between generation and demand causes the system frequency to deviate from the nominal value. Unlimited frequency deviation may drive the system to sectional or complete collapse. In interconnected power systems, power flow and frequency are adjusted by automatic generation control (AGC). AGC includes a load frequency control (LFC) loop and an automatic voltage regulator (AVR) loop. The load frequency control prevents deviations of frequency to achieve zero steady-state errors, and the optimal transient behavior is the target of LFC in a multi-area interconnected power system [1]. In [2] the authors considered the operation between LFC and AVR loops and studied the combinatorial effects between LFC and AVR. In [3], a fuzzy controller is proposed to solve LFC.

Multi-agent systems consist of some autonomous subsystems which are coupled to each other and pursue a common goal. These autonomous subsystems are known as agents. Different agent dynamics as well as different coupling schemes of the agents can create different forms of multi-agent systems. In [4] consensus protocols were studied for agents with single and double integrator dynamics. It was also proved that the proposed consensus protocols reach asymptotic consensus even in the presence of constant disturbances.

In the centralized controller, the implementation of a decision making mechanism is easier as information is collected in a central point [5]; however, it stops execution for each error in the prediction process or information transition channels [6]. Then, it might be seriously subjected to overall failure under islanding [7]. The distributed control is the only possible control strategy in many large-scale systems when communications are limited. One important class of large-scale systems are power systems in which the distributed control can be employed in AGC and frequency controllers [8]. In general, because of load and generation changes, a proportional frequency controller

Received: 04 July. 2016
Revised: 17 Dec. 2016 and 03 Jan. 2107
Accepted: 23 Jan. 2017
∗Corresponding author:
E-mail: adelakbary@yahoo.com (A. Akbarimajd)
Digital object identifier: 10.22098/joape.2017.2522.1220

cannot converge to the desired reference frequency. Integrators are incorporated to reduce static errors [9]. Automatic frequency controls of power systems are implemented at two inner and outer levels. Although it properly works in most of today's power systems, this control architecture might be an unsuitable choice in newly developed power systems. For example, the large-scale influence of renewable power generation adds generation fluctuations. Therefore, the need for fast control architecture with high local disturbance attenuation capacity increases. The power systems' distributed control might also enable effective islanding control and self-healing properties, even when communication between subsystems is limited or unavailable [10, 11].

Optimal power flow (OPF) calculations create the most efficient power system planning and operation by determining optimal control variables and system quantities [12]. The main objective of OPF can be defined to determine the parameters of power system elements such as generators, capacitor banks, and load tap changers to optimize a certain objective function while fulfilling the physical, operational, and security constraints [13]. In [14] the OPF problem was solved using the particle swarm optimization (PSO) and glowworm swarm optimization (GSO) algorithms as well as in [15], an OPF algorithm is proposed to optimize operational cost.

The growth and complexity of modern electric power systems along with the increase in power demand have forced the use of intelligent control systems. The researchers still work on the optimization of controller parameters to achieve a better performance of the system [16]. The Grey Wolf Optimizer (GWO) algorithm mimics the grey wolves' behavior in searching and hunting for prey. The main steps of grey wolf hunting are encircling and harassing the prey. They prefer to live in groups of 5-12 on average [17]. In [18] using the GWO algorithm, parameters of PID controllers were optimized in a three-area system, and it was shown that load frequency control was successful by PID controller tuned by the GWO algorithm.

The aim of this paper is to design an optimal distributed multi-agent controller for load frequency control and OPF. A designed optimal distributed controller and three types of controllers including centralized controller, decentralized controller, and optimal centralized controller are employed for load frequency control in the IEEE 30-bus test system. The performances of decentralized and distributed controllers are compared with those of the two centralized controllers. Controller parameters are optimized using GWO algorithm. In the optimal centralized controller and optimal distributed controller, the objective function was considered to achieve the objective of load frequency control as well as minimize power generation. The controller of each generator is considered as one agent. The controllers of agents are implemented in a distributed manner, that is, the control rule of each agent depends on the agent's state and the states of its neighbors. The proposed approach is tested on an IEEE 30-bus standard system with six generators. Simulation results using MATLAB/SIMULINK show that while there is no global information of system in the optimal distributed controller, it has suitably reduced frequency deviation and power is generated as optimal in the three scenarios of load increase, load reduction, and generator outage.

2. POWER SYSTEM MODEL

In this paper, load frequency control is tested on the IEEE 30-bus test system. The single-line diagram of the test system is shown in Fig. 1. There are synchronous generators in buses 1, 2, 13, 22, 23 and 27, and the other buses are considered as synchronous motor. The difference between our system and the one in [19] is that assumed that there is a generator in each bus.

The power system is modeled by a graph where v and e denote buses (nodes) and lines between the buses (edges), respectively. Each bus is considered as a node that exhibits the swing equation, shown as [9]:

$$m_i \ddot{\delta}_i + d_i \dot{\delta}_i = -\sum_{i \in N_i} K_{ij} \sin(\delta_i - \delta_j) + P_i^m + u_i \quad (1)$$

Where, δ_i, m_i and d_i are demonstrated as the phase angle, inertia coefficient, and damping coefficient for bus i, respectively. p_i^m and u_i are the power of bus i and the mechanical input of bus i, respectively. N_i is the set of neighboring buses of bus i. Injected power is defined to be positive and loads are defined to be negative. K_{ij} is given in Eq. (2):

$$K_{ij} = |V_i||V_j||b_{ij}| \quad (2)$$

Where, V_i is the voltage of bus i and b_{ij} is the susceptance of line (i, j). By linearizing Eq. (1) in the equilibrium point where $\delta_i = \delta_j \forall i, j \in v$, the linearized swing equation is given in Eq. (3) [17]:

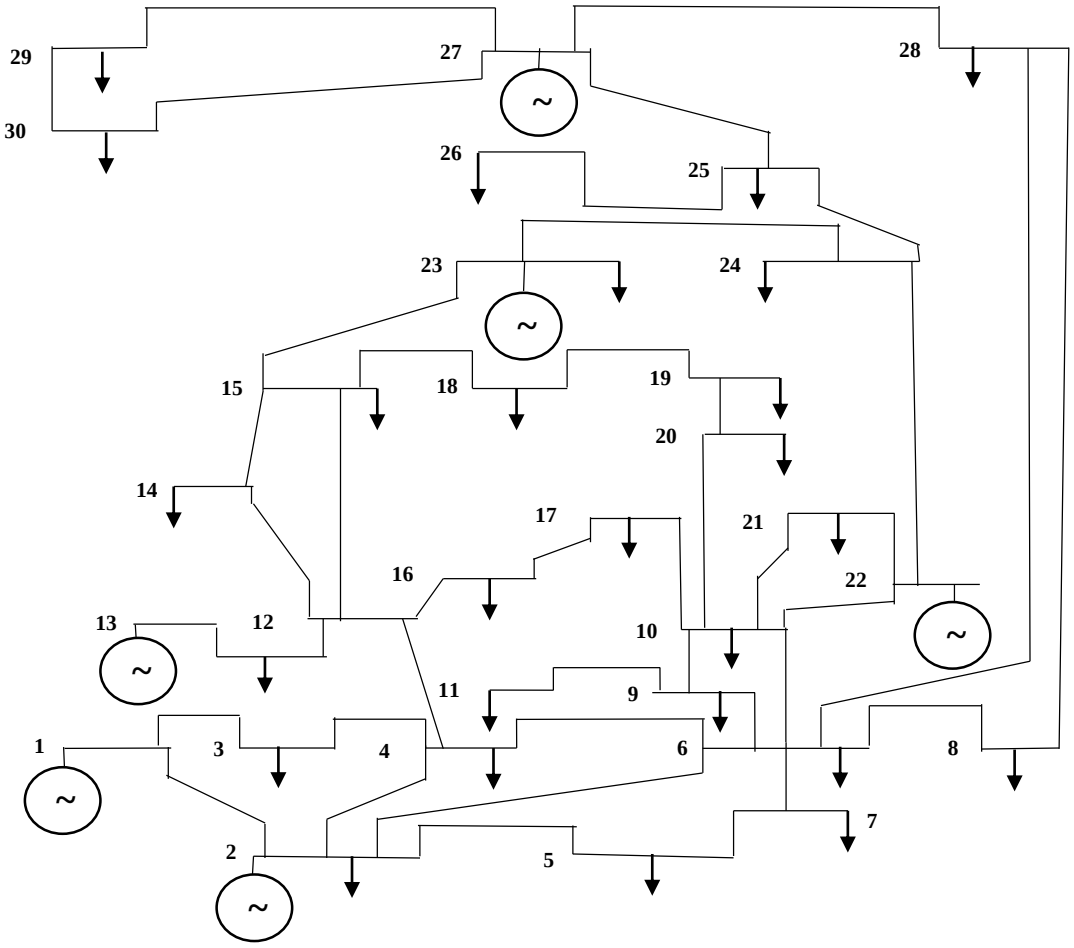

Fig. 1. Single line diagram of the IEEE 30 bus test system.

$$m_i \ddot{\delta}_i + d_i \dot{\delta}_i = -\sum_{i \in N_i} K_{ij}(\delta_i - \delta_j) + P_i^m + u_i \quad (3)$$

It is noteworthy that as our goal is to focus on controller design and study the difference among performance of various control structures including centralized, decentralized and distributed control structures, we employ a simple model in our studies. That is we ignore the dynamics of turbine and we do not apply external change in mechanical load. In fact the control signal u_i is mechanical input and changes the power inside the control loop and we do not have any other mechanical change outside of control loop.

3. CONTROLLER STRUCTURES

Frequency control is used to guarantee the frequency convergence of buses toward the reference frequency. In [20], several classes of multi-agent control systems are considered whose common property is the dependence of the dynamics of each agent on the agent's state and the states of its neighboring agents. The optimal distributed controller is designed, and load frequency control and OPF are studied for the optimal distributed controller and optimal centralized controller. LFC is also studied using two types of centralized controller and decentralized controller.

3.1. Optimal distributed controller

In this controller, the local frequency is compared with a global reference frequency, and the power generation marginal cost is compared with the controller's neighboring buses. In other words, the optimal distributed control pursues the aim of satisfying the following conditions:

Condition 1: The controller regulates the bus frequencies to the reference frequency, i.e.

$$\lim_{t \to \infty} W_i(t) = W^{ref} \; \forall i \in v \quad (4)$$

Condition 2: The power generation minimizes the generation cost in steady state, i.e.

$$\lim_{t \to \infty} u(t) = u^* \quad (5)$$

The distributed control protocol is given as

$$u_i = \alpha(\hat{W}_i - W_i) \tag{6}$$

$$\dot{\hat{W}} = \beta(\sum_{j\in N_i} K_{ij}\alpha(C_j(\hat{W}_j - W_j) - C_i(\hat{W}_i - W_i))) + \gamma(W^{ref} - W_i) \tag{7}$$

u_i is power generation by each generator and W is frequency. $\hat{W}$ is part of the integral of the controller, and C is the power generation cost in each generator. The optimal distributed controller architecture is shown in Fig. 2 where C_1 to C_n show controller in each bus [20].

This controller consists of a proportional and an integral

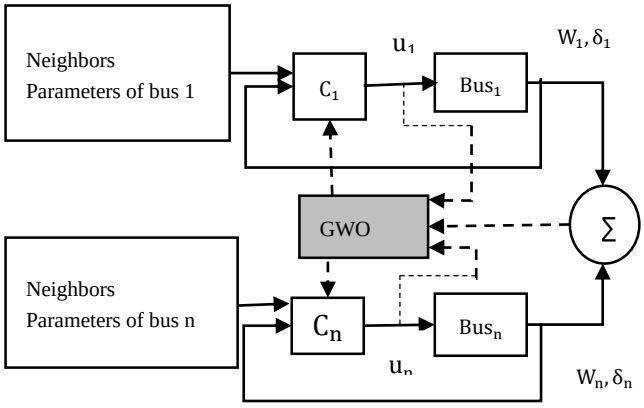

Fig. 2. Optimal distributed control architecture.

part. In the integral part, the local frequency is compared with nominal frequency and its neighbor frequency, while the cost of power generation is compared with neighboring buses. In the proportional part, frequency is compared to $\hat{W}$ in each bus. α, β and γ parameters regulate.

3.2. Other possible control structures

3.2.1. Centralized controller

A centralized frequency control protocol is designed for power systems. The proportional controller of bus i is given as

$$u_i = \alpha(\hat{W} - W_i) \tag{8}$$

$\hat{W}$ is the integral part of the controller and has the following dynamics:

$$\dot{\hat{W}} = \beta(W^{ref} - \frac{1}{n}\sum_{i\in v} W_i) \tag{9}$$

It is assumed that the average frequency of the buses is measured by the central controller. The architecture of the centralized controller is shown in Fig. 3 [20].

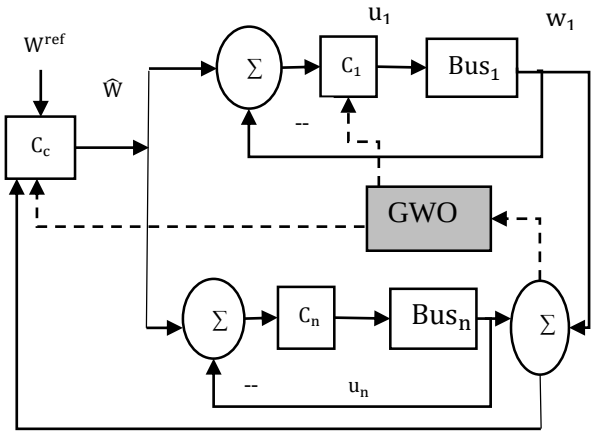

Fig. 3. Centralized control architecture.

In Fig. 3, C_c is the integral part, considered as the central controller where all the frequency and reference frequency enter, and which compares the average frequency to reference frequency. C_1 to C_n are the proportional part of the controller and compare frequency to $\hat{W}$. α and β parameters regulate.

3.2.2. Decentralized controller

In the decentralized controller, each bus is controlled based on its own state. In the decentralized control there is no need to send control signals or reference values from one bus to other buses. The controller of bus i is given as:

$$\dot{Z}_i = W^{ref} - W_i \tag{10}$$

$$u_i = \alpha(W^{ref} - W_i) + \beta Z_i \tag{11}$$

The decentralized controller's architecture is shown in Fig. 4 [20].

In Fig. 4, C_1 to C_n consist of proportional and integral parts. Frequency is compared with reference frequency in the integral part, and difference between reference frequency and frequency is summed with the integral part in the proportional part. α and β parameters regulate.

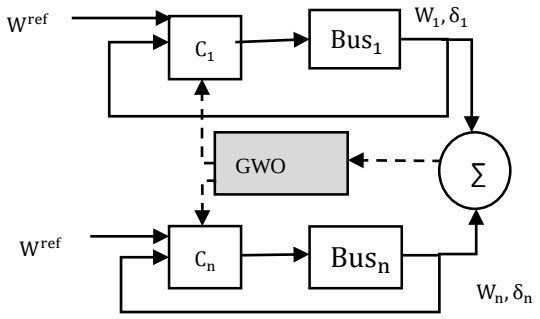

Fig. 4. Decentralized control architecture.

3.2.3. Optimal centralized controller

In the optimal centralized controller, the previously mentioned conditions are satisfied as well. In the optimal centralized control, in addition to frequency convergence to the constant reference frequency, an objective function of power generation is minimized. The centralized control rule is given as

$$u_i = \alpha(\hat{W}_i - W_i) \tag{12}$$

$$\dot{\hat{W}}_i = \beta(u^* - \alpha(\hat{W}_i - W_i)) + \gamma(W^{ref} - W_i) \tag{13}$$

where u^* is minimized using:

$$\sum_{i \in v} \frac{1}{2} C_i u_i^2 \tag{14}$$

The optimal centralized controller's architecture is shown in Fig. 5 [20].

In Fig. 5, C_c is the central controller that generated power by all generators and power generation cost receive and sends u^* to all controllers using Eq. (14). C_1 to C_n are the controllers of each generator, consisting of proportion and integral parts. α, β and γ parameters regulate.

4. GREY WOLF OPTIMIZER

The GWO algorithm is expanded by Mirjalili et al. [17]. This algorithm reflects the grey wolves' behavior. Grey wolves prefer to live in a group of 5-12 members on average. They have a very hard social dominant hierarchy. The group leaders are a male and a female. There are four classifications in the group, alpha (α), beta (β), delta (δ), and omega *(ω)*. Alpha is the first level of classification and is responsible for making decisions more than all others. The powerful member of

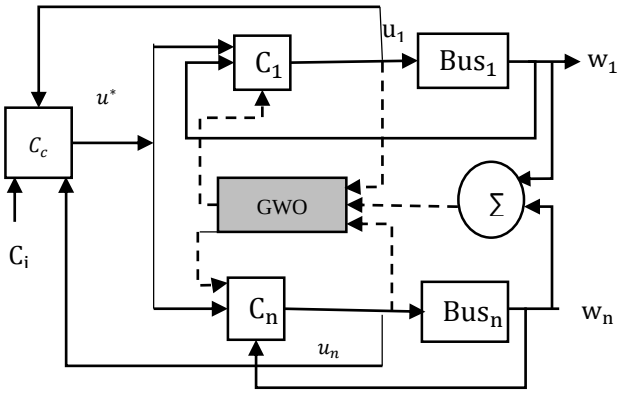

Fig. 5. Optimal Centralized control architecture.

the group is not necessarily alpha, but it is the best in group management. This classification shows that organization and discipline are more important in a group than strength. Beta is the second level of classification in the group. Beta wolves help the alpha member in making decisions and other actions. In the absence of the alpha, beta can assume the responsibility of the group. The beta wolf fortifies the command of alpha all over the group. Delta is the third level of classification including scouts, sentinels, hunters, and caretakers. The lowest classification of the group is omega. Omega wolves have to surrender to all the dominant wolves. They are allowed to have last of all. The main steps of grey wolf hunting are encircling and harassing the prey [18].

In [15], the two main steps of hunting are formulated. The encircling behavior is given in Eqs. (15) and (16):

$$\vec{D} = \left| \vec{C}.\vec{X}_p(t) - \vec{X}(t) \right| \tag{15}$$

$$\vec{X}(t+1) = \left| \vec{X}_p(t) - \vec{A}.\vec{D} \right| \tag{16}$$

where t demonstrates the current iteration, $\vec{A}$ and $\vec{C}$ are coefficient vectors, $\vec{X}_p$ is the position vector of the prey and $\vec{X}$ demonstrates the position vector of a grey wolf. $\vec{A}$ and $\vec{C}$ vectors are given in Eqs. (17) and (18):

$$\vec{A} = 2\vec{a}.\vec{r}_1 - \vec{a} \tag{17}$$

$$\vec{C} = 2.\vec{r}_2 \tag{18}$$

where $\vec{\alpha}$ is linearly decreased from 2 to 0, and r_1, r_2 are random vectors in [0, 1].

Although there is no optimal location in an abstract search space, the hunting behavior of grey wolves is

simulated assuming that alpha, beta, and delta have a better knowledge about the potential location of the prey. The corresponding relations are given in Eqs. (19), (20), and (21):

$$\vec{D}_\alpha = \left|\vec{C}_1.\vec{X}_\alpha - \vec{X}\right|, \vec{D}_\beta = \left|\vec{C}_2.\vec{X}_\beta - \vec{X}\right| \\ , \vec{D}_\delta = \left|\vec{C}_3.\vec{X}_\delta - \vec{X}\right| \quad (19)$$

$$\vec{X}_1 = \vec{X}_\alpha - \vec{A}_1.(\vec{D}_\alpha), \vec{X}_2 = \vec{X}_\beta - \vec{A}_2.(\vec{D}_\beta) \\ , \vec{X}_3 = \vec{X}_\delta - \vec{A}_3.(\vec{D}_\delta) \quad (20)$$

$$\vec{X}(t+1) = \frac{\vec{X}_1 + \vec{X}_2 + \vec{X}_3}{3} \quad (21)$$

Moreover, alpha, beta, and delta estimate the position of the prey, and other wolves update their positions randomly around the prey.

Grey wolves finish the hunting by attacking the prey, which is applicable when the prey stops moving. a decreases from 2 to 0 for mathematically model approaching the prey. Grey wolves update their position based on the location of the alpha, beta, and delta. Grey wolves diverge to search for the prey, and approach each other to attack the prey. $\vec{A}$ is a random value in the distance $[-2a, 2a]$. $|A| \succ 1$ wolves diverge from the prey to find a fitter prey, and $|A| \prec 1$ models the attack on the prey. C randomly gives the prey a weight, making it more difficult for the wolves to reach the prey.

To sum up, the search process starts for grey wolves by providing a random population. Alpha, beta, and delta wolves estimate the position of the prey in each iteration. Parameter *a* decreases to emphasize exploration and exploitation from 2 to 0, respectively. Wolves diverge from the prey when $|A| \succ 1$ and converge towards the prey when $|A| \prec 1$. Finally, the GWO algorithm is terminated by the satisfaction of a criterion [17].

Load is increased by the steps of 0.02p.u in 2, 3 and 7 buses at the times of 1, 2, and 3 sec, respectively, and then the parameters of controllers are optimized. The cost function in the optimization of the centralized and decentralized controllers is considered as:

$$\min \sum \Delta w_i \quad (22)$$

where $\Delta\omega_i$ is frequency deviation. α and β are regulated by GWO in the centralized and decentralized controllers.

Optimization in the optimal centralized and optimal distributed controllers is performed using the following cost function:

$$\min(\sum \Delta w_i + \sum C_i u_i) \quad (23)$$

Then α, β and γ parameters are regulated by GWO in these two controllers. Generation cost is calculated according to $\sum C_i u_i^2$ for all generators.

5. SIMULATION RESULTS

The IEEE 30-bus test system is simulated in the MATLAB/Simulink. The parameters of generators of the test system are given in Table 1, and optimized parameters are presented in Table 2. Power load is increased by steps of 0.02 p. u in the 2, 3 and 7 buses at the times of 1, 2, and 3 sec, respectively. Models of centralized, decentralized, optimal centralized, and optimal distributed controllers are used to achieve a better dynamic behavior and minimize power generation costs. Studies are conducted in three scenarios including load increase, load reduction, and generator outage.

Table1. Generator data of IEEE 30-bus test system.

Unite	bus	C($/MWh^2$)	$U_{max}(pu)$	$U_{min}(pu)$
G1	1	0.0200	0.5646	-0.085
G2	2	0.0175	0.1903	-0.459
G3	13	0.0250	0.1300	-0.270
G4	22	0.0625	0.2841	-0.115
G5	23	0.0250	0.1080	-0.142
G6	27	0.0083	0.2809	-0.169

Table 2. Controller parameters.

controller	α	β	γ
centralized	3.0923	3.2605	-
decentralized	2.6595	101.5913	-
Optimal centralized	2.4991	1.0065e-04	49.2705
Optimal distributed	2.5280	1.8181e-04	40.3141

5.1. Scenario 1: Load increasing

In this scenario, load is increased in the 4, 17, and 27 buses by the steps of 0.02p.u at the times of 1, 5, and 10 sec. the frequency deviation and generation power of generators are shown in Figs 6-13. The generated power in each bus and generation cost are presented in Table 3, and values of evaluation indicators are given in Table 4.

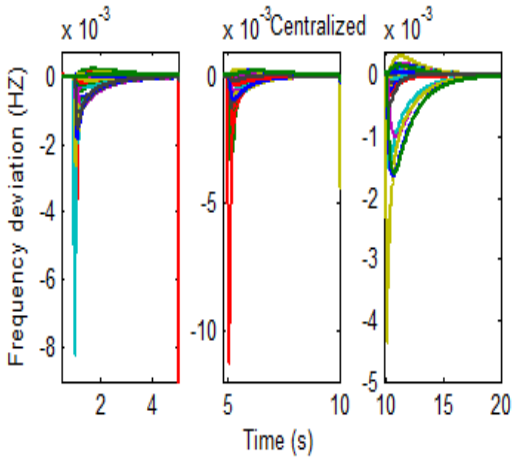

Fig. 6. Frequency deviation under centralized controller in scenario of load increase.

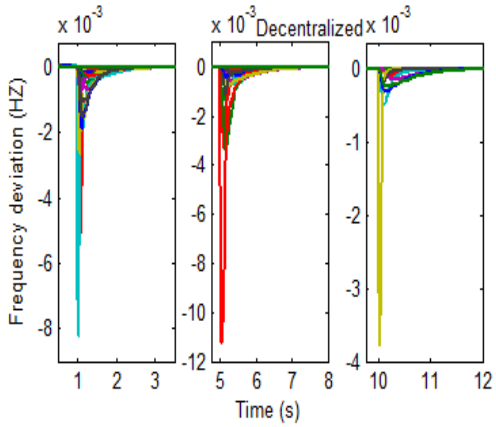

Fig. 7. Frequency deviation under decentralized controller in scenario of load increasing.

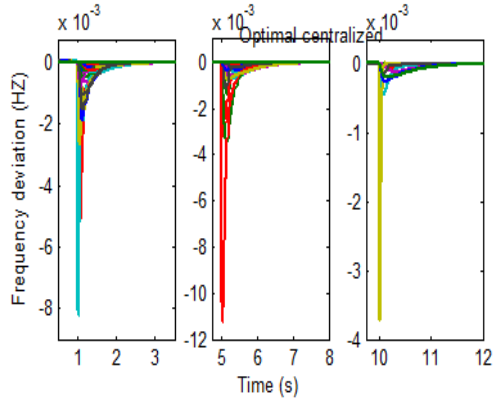

Fig. 8. Frequency deviation under optimal centralized controller in scenario of load increasing.

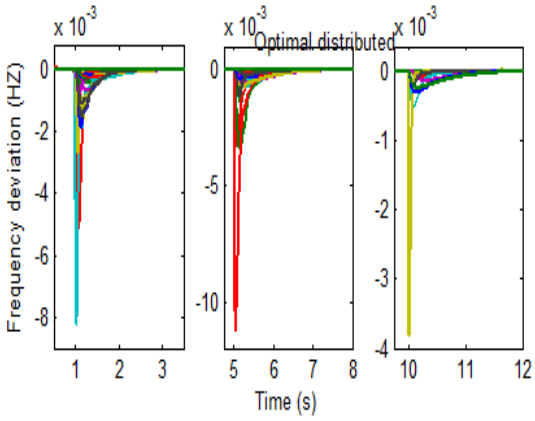

Fig. 9. Frequency deviation under optimal distributed controller in scenario of load increasing.

The settling time is limited to 17.4089, 11.4237, 11.3223, and 11.4358 sec for centralized, decentralized, optimal centralized, and optimal distributed controllers, respectively. Figures 6 and 7 show that the decentralized controller reduces the settling time more than the centralized controller.

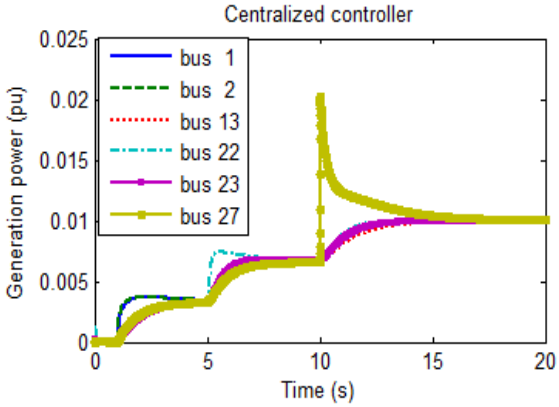

Fig. 10. Generation power under centralized controller in scenario of load increasing.

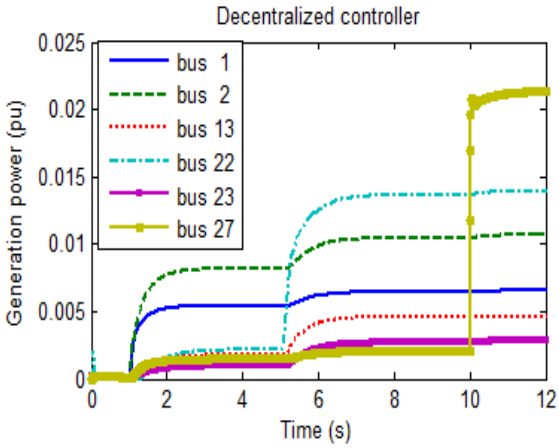

Fig. 11. Generation power under decentralized controller in scenario of load increasing.

Table 3. Change of generation power in the each bus and generation cost for scenario of load increasing.

Generation power	Bus 1 (pu)	Bus 2 (pu)	Bus 13 (pu)	Bus 22 (pu)	Bus 23 (pu)	Bus 27 (pu)	Generation cost ($/h)
centralized	0.01	0.01	0.01	0.01	0.01	0.01	0.01583
decentralized	0.006532	0.01067	0.004653	0.01394	0.002838	0.02137	0.01952
Optimal centralized	0.006388	0.0108	0.004624	0.01395	0.002757	0.0215	2.611e-03
Optimal distributed	0.006535	0.01068	0.004655	0.01392	0.002843	0.02137	2.599e-03

Table 4. Calculation of evaluation indicators for scenario of load increasing.

	Under shoot (pu)	Settling time (s)
centralized	0.0113	17.4089
decentralized	0.0113	10.4237
Optimal centralized	0.0113	10.3223
Optimal distributed	0.0113	10.4358

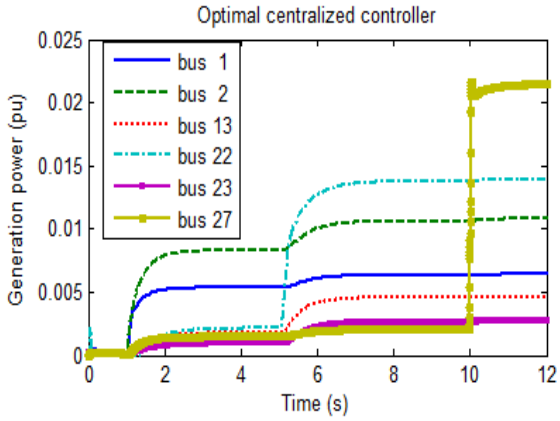

Fig. 12. Generation power under optimal centralized controller in scenario of load increasing.

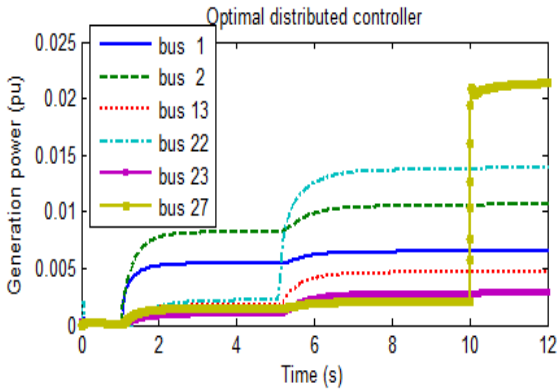

Fig. 13. Generation power under optimal distributed controller in scenario of load increasing.

In the centralized controller, control powers are generated equally in all generators, while they are generated unequally to the locations of disturbances in the decentralized controller. The control power is generated in each bus based on the locations of disturbances as well as considering minimum generation cost in both optimal centralized and optimal distributed controllers. The generation cost is obtained as 2.611e-03 and 2.599e-03 for optimal centralized and optimal distributed controllers, respectively.

Figure 14 shows the comparison between the worst settling times of buses in four types of controllers in the scenario of load increase.

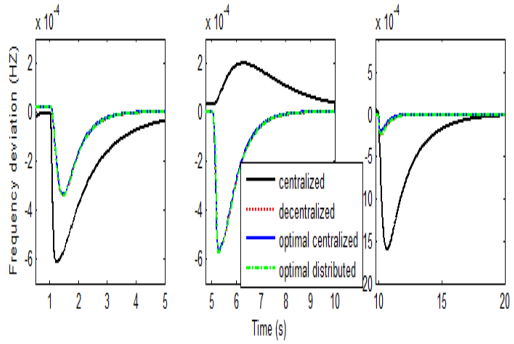

Fig. 14. Comparison the worst settling time of buses in the four kinds of controller.

Figure 14 shows that the distributed controller suitably regulates settling time.

5.2. Scenario 2: Load reduction

In this scenario**,** load is decreased in the 7, 23, and 26 buses by the steps of -0.02p.u at the times of 1, 5, and 10 sec. The frequency deviation and generation power of generators are shown in Figs. 15-22. Power reduction in each bus and generation costs are presented in Table 5, and the calculations of evaluation indicators are given in Table 6.

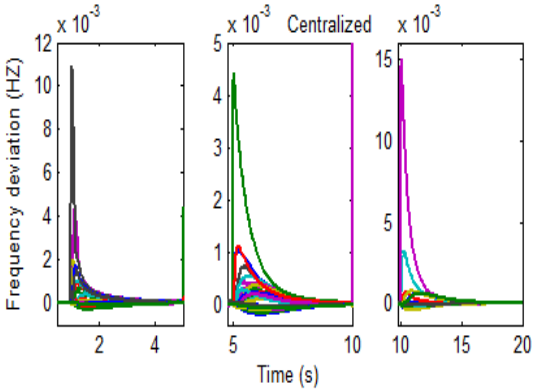

Fig. 15. Frequency deviation under centralized controller in scenario of load reduction.

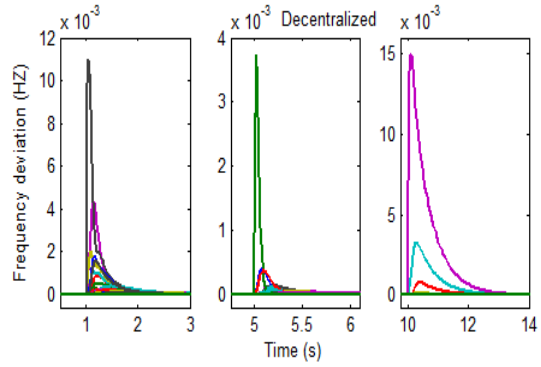

Fig. 16. Frequency deviation under decentralized controller in scenario of load reduction.

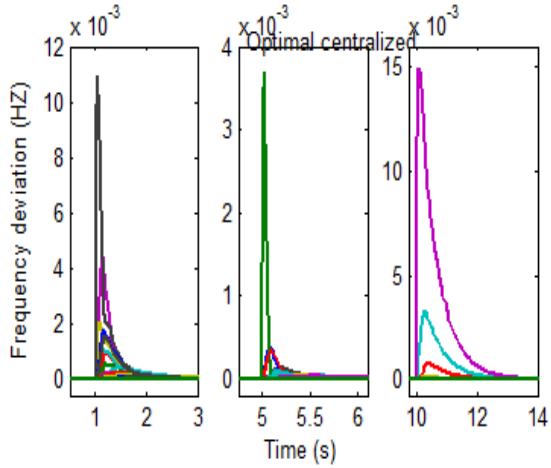

Fig. 17. Frequency deviation under optimal centralized controller in scenario of load reduction.

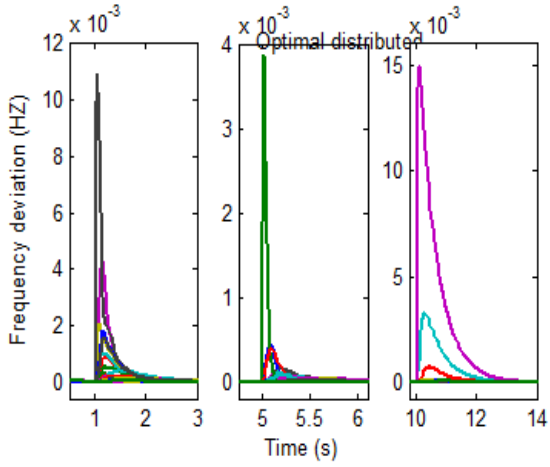

Fig. 18. Frequency deviation under optimal distributed controller in scenario of load reduction.

The settling time is obtained as 16.7591, 12.6987, 12.6929, and 12.6866 sec for the centralized, decentralized, optimal centralized, and optimal distributed controllers in the frequency deviation, respectively.

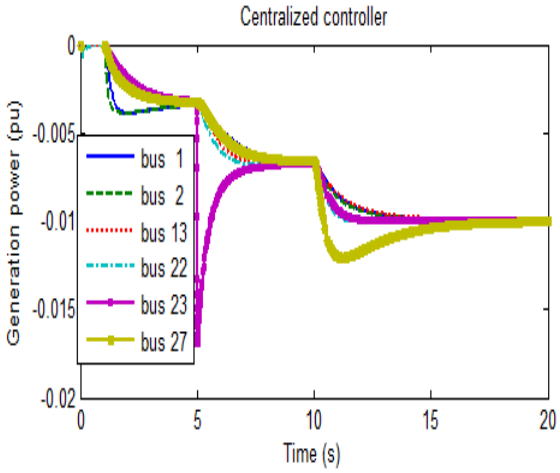

Fig. 19. Generation power under centralized controller in scenario of load reduction.

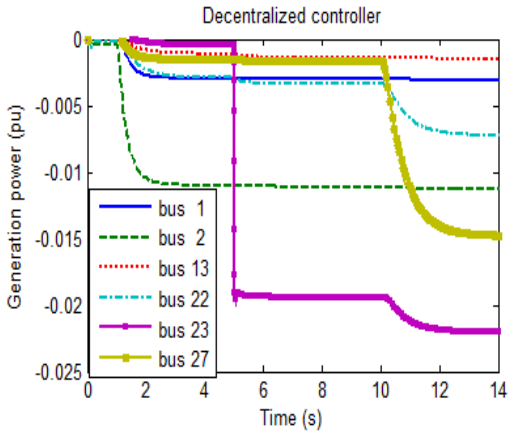

Fig. 20. Generation power under decentralized controller in scenario of load reduction.

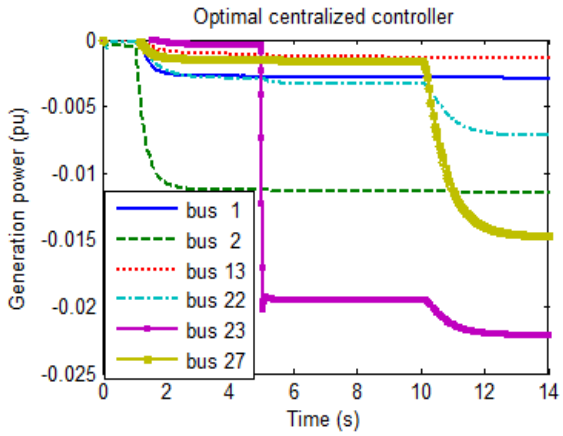

Fig. 21. Generation power under optimal centralized controller in scenario of load reduction.

Table 5. Change of generation power in the each bus and generation cost for scenario of load reduction.

Generation power	Bus 1 (pu)	Bus 2 (pu)	Bus 13 (pu)	Bus 22 (pu)	Bus 23 (pu)	Bus 27 (pu)	Generation cost ($/h)
centralized	-0.01	-0.01	-0.01	-0.01	-0.01	-0.01	0.01583
decentralized	-0.003106	-0.01133	-0.001491	-0.007249	-0.02203	-0.01479	0.01973
Optimal centralized	-0.002903	-0.01151	-0.001409	-0.007245	-0.02217	-0.01474	2.654e-03
Optimal distributed	-0.003114	-0.01132	-0.001492	-0.007236	-0.02204	-0.0148	2.630e-03

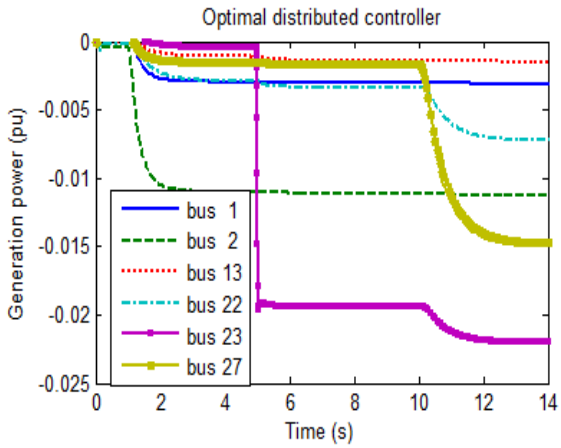

Fig. 22. Generation power under optimal distributed controller in scenario of load reduction.

Control powers in the centralized controller are reduced equally in the all generators. Generation cost is obtained as 2.654e-03 and 2.630e-03 for optimal centralized and optimal distributed controllers, respectively.

Table 6. Calculation of evaluation indicators for scenario of load reduction.

	Over shoot (pu)	Settling time (s)
centralized	0.0150	16.7591
decentralized	0.0150	12.6987
Optimal centralized	0.0150	12.6929
Optimal distributed	0.0150	12.6866

5.3. Scenario 3: Generator outage

In this scenario, generator 23 exits at the time of 1 sec. Generation power in bus 23 is 0.192p.u. The frequency deviation and generation power of generators are shown in Figs 23-30. Generation power in each bus and generation cost are presented in Table 7, and evaluation indicators are given in Table 8.

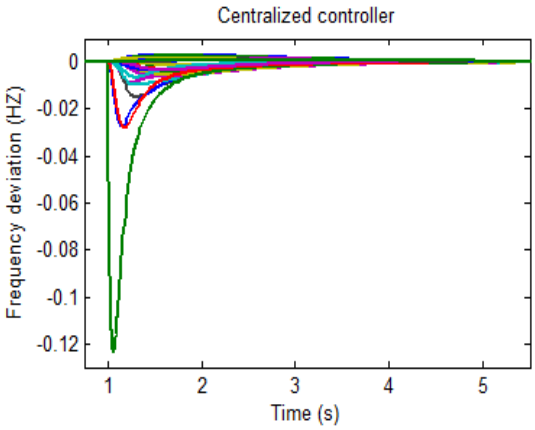

Fig. 23. Frequency deviation under centralized controller in scenario of generator outage

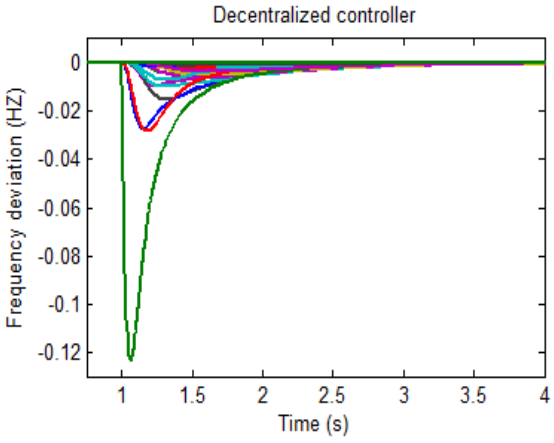

Fig. 24. Frequency deviation under decentralized controller in scenario of generator outage

Table 7: Change of generation power in the each bus and generation cost for scenario of generator outage

Generation power	Bus 1 (pu)	Bus 2 (pu)	Bus 13 (pu)	Bus 22 (pu)	Bus 23 (pu)	Bus 27 (pu)	Generation cost ($/h)
centralized	0.0384	0.0384	0.0384	0.0384	0	0.0384	1.966
decentralized	0.009112	0.01608	0.05119	0.09048	0	0.02514	5.886
Optimal centralized	0.008745	0.01597	0.05118	0.09109	0	0.02504	7.937e-02
Optimal distributed	0.009128	0.01611	0.05122	0.09036	0	0.02517	7.832e-02

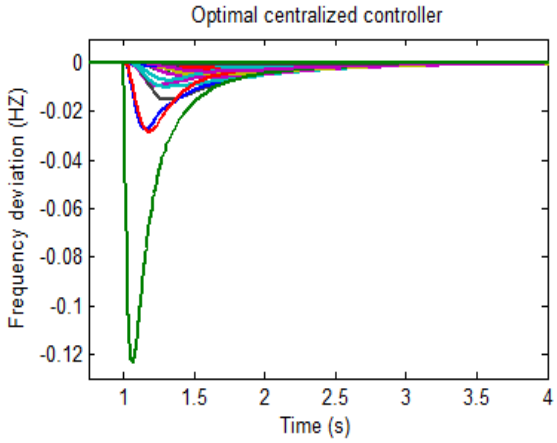

Fig. 25. Frequency deviation under optimal centralized controller in scenario of generator outage

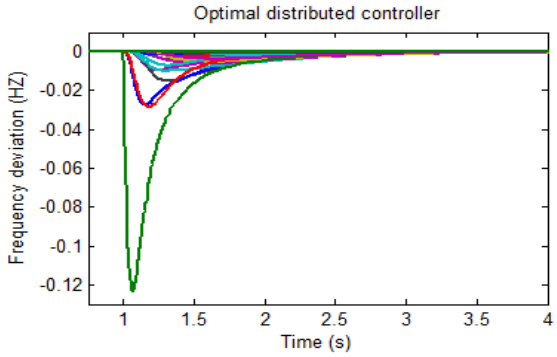

Fig. 26. Frequency deviation under optimal distributed controller in scenario of generator outage

The settling time is limited to 4.0849, 2.7981, 2.7886, and 2.7978 sec for centralized, decentralized, optimal centralized and optimal distributed controllers, respectively.

Other generators are compensated generation power that the generator of bus 23 had been generated. Control powers in the centralized controller are generated equally in all generators. Power generation is obtained based on the locations of disturbances and to minimize generation cost in the optimal centralized and optimal distributed controllers.

Table 8. Calculation of evaluation indicators for scenario of generator outage

	Under shoot (pu)	Settling time (s)
Centralized	0.1234	4.0849
Decentralized	0.1234	2.7981
Optimal centralized	0.1234	2.7886
Optimal distributed	0.1234	2.7978

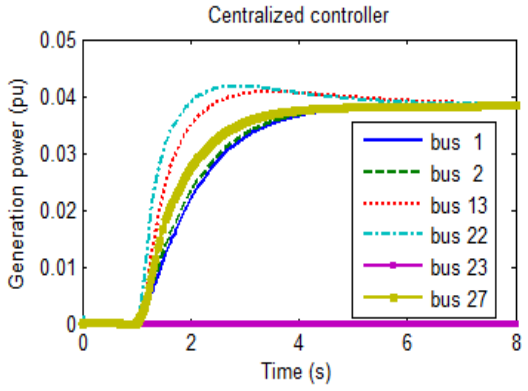

Fig. 27. Generation power under centralized controller in scenario of generator outage

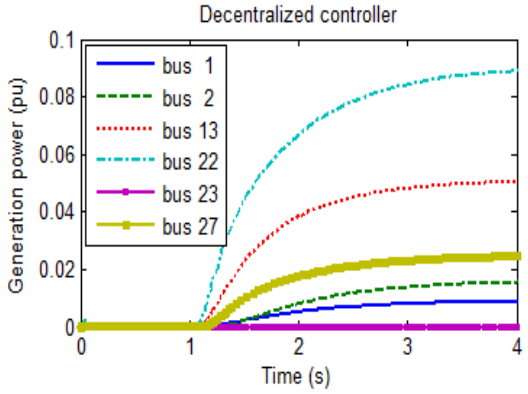

Fig. 28. Generation power under decentralized controller in scenario of generator outage

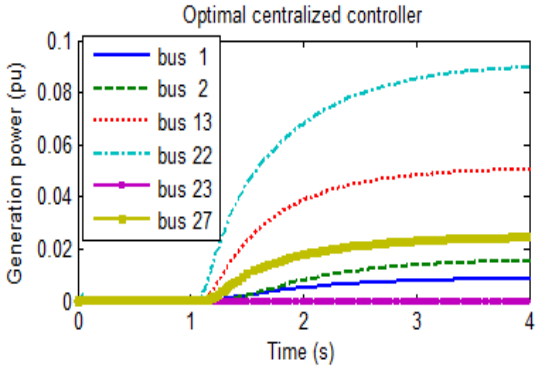

Fig. 29. Generation power under optimal centralized controller in scenario of generator outage

Results show that the optimal distributed controller has suitably reduced frequency deviation and generation cost in the three scenarios of load increase, load reduction, and generator outage.

6. CONCLUSIONS

In this paper, an optimal distributed controller is designed for optimal load frequency control. The optimal distributed controller and three types of controllers including centralized, decentralized, and optimal centralized controllers were applied for load frequency

control in the IEEE 30-bus test system.

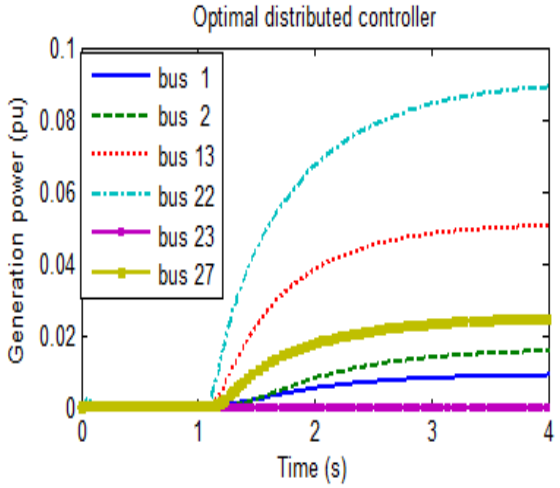

Fig. 30. Generation power under optimal distributed controller in scenario of generator outage

In the optimal distributed and optimal centralized controllers, in addition to the objective of load frequency control, the objective of minimizing a cost function was considered to minimize the power generation cost of generators. Results were studied in three scenarios of load increase, load reduction, and generator outage. Results demonstrated that the performance of decentralized controller is better than that of the centralized controller. Both optimal centralized and optimal distributed controllers reduce power generation costs in the generators. The optimal distributed controller has suitably reduced frequency deviation and generation cost in the three scenarios of load increase, load reduction, and generator outage, while there is no global information of system in the optimal distributed controller. Advantage of the proposed controller is in its distributed structure. Disturbed controllers are advantageous in terms of fault tolerance, low data exchange, decrease in communication channel, low delay time etc. Nevertheless, distributed controllers are subject to decrease in performance in compression to centralized controllers. Simulations show that the performance of the controller in terms of overshoot and settling time has not been degraded.

References

[1] G. Gross, and J. W. Lee "Analysis of load frequency control performance assessment criteria," *IEEE Trans. Power Syst.*, vol. 16, no. 3, pp. 520-525, 2001.

[2] S. Satyanarayana, R. K. Sharma, A. Mukta, and S. A. Kumar, "Automatic Generation control in power plant using PID, PSS and fuzzy-PID controller," *Smart Electr. Grid*, pp. 1-8, 2014.

[3] O. Abedinia, N. Amjady, A. Ghasemi, and H. Shayeghi "Multi-stage fuzzy load frequency control based on multi-objective harmony search algorithm in deregulated environment," *J. Oper. Autom. Power Eng.*, vol. 1, no. 1, pp. 63-73, 2013.

[4] M. Andreasson, H. Sandberg, D. Dimarogonas, and K. Johansson, "Distributed Integral Action: Stability Analysis and Frequency Control of Power Systems," *51st IEEE Conf. Decis. Control*, pp. 2077- 2083, 2012.

[5] E. Planas, A. Gil-de-Muro, J. Andreu, I. Kortabarria, and I. Martinez de Alegria, "General aspects, hierarchical controls and droop methods in micro grids: a review," *Renew. Sustain. Energy Rev.*, pp. 147-159, 2013.

[6] A. Del Barrio, S. Memik, M. Molina, J. Mendias, and R. Hermida, "A Distributed controller for Managing Speculative Functional Units in High Level Synthesis," *IEEE Trans.-Aided Des. Integr. Circuits Syst.*, vol. 30, pp. 350-363, 2011.

[7] F. Katiraei, M. Iravani, and P. Lehn "Micro-grid autonomous operation during and subsequent to islanding process," *IEEE Trans. Power Delivery*, vol. 20, no. 1, pp. 248-257, 2005.

[8] F. Liu, Y. H. Song, J. Ma, S. Mei, and Q. Lu, "Optimal load-frequency control in restructured power systems. Generation," *IEE Proc.-Gener., Transm. Distrib.*, vol. 150, no. 1, pp. 87-95, 2003.

[9] J. Machowski, J. W. Bialek, and J. R. Bumby "Power system dynamics: stability and control," *Wiley*, 2008.

[10] N. Senroy, G. T. Heydt, and V. Vittal "Decision tree assisted controlled islanding," *IEEE Trans. Power Syst.*, vol. 21, no. 4, pp. 1790-1797, 2006.

[11] B. Yang, V. Vittal, and G.T Heydt "Slow-coherency-based controlled islanding: A demonstration of the approach on the august 14, 2003 blackout scenario," *IEEE Trans. Power Syst.*, vol. 21, no. 4, pp. 1840-1847, 2006.

[12] Momoh JA, Zhu JZ "Improved interior point method for OPF problems," *IEEE Trans. Power Syst.*, vol. 14, no. 3, pp. 1114-1120, 1999.

[13] K. Abaci and V. Yamacli "Differential search algorithm for solving multi-objective optimal power flow problem," *Int. J. Electr. Power Energy Sys.*, vol. 79, pp. 1-10, 2016.

[14] S. Surender Reddy and C. Srinivasa Rathnam "Optimal Power Flow using Glowworm Swarm Optimization," *Int. J. Electr. Power Energy Syst.*, vol. 80, pp. 128-139, 2016.

[15] S. Derafshi Beigvand, and H. Abdi "Optimal power flow in the smart grid using direct load control program," *J. Oper. Autom. Power Eng.*, vol. 3, no. 2, pp. 102-115, 2015.

[16] R. Sahu, S. Panda, and U. Rout, "DE optimized parallel 2-DOF PID controller for load frequency control of power system with governor dead-band nonlinearity," *Int. J. Electr. Power Energy Syst.*, vol. 49, pp. 19-33, 2013.

[17] S. Mirjalili, S. Mirjalili, and A. Lewis "Grey Wolf Optimizer," *Adv. Eng. Software*, vol. 69, pp. 46-61, 2014.

[18] Y. Sharma, and L. Saikia, "Automatic generation control of a multi-area ST-Thermal power system using Grey Wolf Optimizer algorithm based classical controllers," *Int. J. Electr. Power Energy Syst.*, vol. 73, pp. 853-862, 2015.

[19] M. Andreasson, D. Dimarogonas, H. Sandberg, and K. Johansson "Distributed Control of Networked Dynamical Systems: Static Feedback, Integral Action and Consensus," *IEEE Trans. Autom. Control*, vol. 59, no. 7, pp. 1750-1764, 2014.

[20] M. Andreasson, "Control of Multi-Agent Systems with Applications to Distributed Frequency Control Power Systems," [Thesis]. *Stockholm: KTH R. Inst. Technol.*, 2013.